CURRENT METHODOLOGY AT THE BUREAU OF RECLAMATION FOR THE NONLINEAR ANALYSES OF ARCH DAMS USING EXPLICIT FINITE ELEMENT TECHNIQUES

Barbara Mills-Bria, P.E.,[1] Larry Nuss, P.E.[2] and Dr. Anil Chopra[2]

[1] *Bureau of Reclamation, Structural Engineernver, Colorado, USA, bmills@do.usbr.gov.*
[2] *Bureau of Reclamation, Structural Engineer; Colorado, USA; lnuss@do.usbr.gov.*
[3] *Professor; Department of Civil Engineering, University of California; chopra@ce.berkeley.edu.*

ABSTRACT :
The Bureau of Reclamation is using explicit finite element techniques to perform static and seismic non-linear structural analysis of concrete dams. The analyses presented are for a 500-foot-high thick arch dam in a wide canyon and a 260-foot-high thin arch dam in a narrow canyon. The thick arch dam has 160,000 nodes, 26 contraction joints and a potentially moveable foundation block. The reservoir upstream from the older arch dam and the water between the dams is modeled with fluid finite elements. The fluid elements provide hydrostatic and hydrodynamic interactions for this complex condition. Contact surfaces capable of sliding and opening represent the contraction joints, unbonded lift lines, foundation discontinuities, and interfaces between the dam, foundation, and reservoir. Non-reflecting boundaries are at the foundation and reservoir extents. Deconvolved ground motions are applied at depth in the foundation, propagate up through the foundation and provide spatially varying motions around the canyon. Material properties were obtained from laboratory tests and further calibrated using natural frequencies. Photogrammetry techniques were used for accurate surface topography and foundation bedding plane orientations. The finite element model of the thin arch dam has over 400,000 nodes. There is an older 210-foot-high arch dam just 7 feet upstream that is included in the model. Seasonal thermal loads are applied to the thin arch dam. The program TRUEGRID was used to create the model geometry and LSDYNA was used for the structural analyses.

KEYWORDS:
Non-linear, dam, dynamic, foundation block, seismic, finite element

1. THICK ARCH DAM

Hungry Horse Dam is a concrete gravity arch structure, over 560 feet high and 2100 feet long, completed in 1953. (see Figure 1)

1.1. Foundation Characterization

The dam is founded on dolomitic limestone. The left abutment is formed by a bedding dip slope, such that bedding plane partings underlying the dam and daylight in the natural slopes downstream (see Figure 1). The bedding dips toward the right abutment and slightly upstream. Several continuous open bedding plane partings were identified. Numerous faults and shears were also mapped in the foundation, mostly on the left abutment. A series of prominent joint sets also cuts the foundation rock. In various combinations, the bedding plane partings (base planes), faults and shears (side boundaries), and joints (back release planes) form potentially unstable blocks within the left abutment of the dam. Although the faults and shears offset the bedding plane partings, continuous base planes have been identified (termed “EP” planes) along which different partings (termed “CPP” planes) line up across the faults or step in such a way as to open at the faults as a result of downstream block movement.

Figure 1. General View of Hungry Horse Dam and continuous bedding plane partings - left abutment

Following a 3-D linear elastic finite element model, a coupled 3-D nonlinear dynamic analysis, with the dam and foundation block included in the same model, allowed for load re-distribution and provided a more realistic estimate of the potential for foundation displacement and dam failure. A model was developed using finite element program LS-DYNA (Livermore Software Technology Corporation, 2003. This paper describes this state-of-the-art analysis. This marks the first time that such analyses have been a major component of a decision as to whether or not to modify a dam at the Bureau of Reclamation. Therefore, these analyses were very much a team effort and received both internal and external review. Rather than simply handing a set of material properties and input to the structural analysts, the geologists, geophysicists, and geotechnical engineers assisted with developing and checking the input and evaluating the output and met regularly to discuss the results.

1.2 LS-DYNA Analysis

1.2.1 Finite Element Model

The finite element model used in the nonlinear coupled analyses is shown in Figure 2. The finite elements representing the concrete and rock were modeled as linear elastic materials. The reservoir was also modeled using LaGrangian elements, but with an equation of state representing a fluid. Non-reflecting boundaries were provided at the edges of the model and at the elevation of seismic load application. The finite element model includes all of the vertical contraction joints between the dam monoliths, modeled as contact surfaces (without the shear keys that were actually constructed in the joints). Contact surfaces were also used to model the interface between the dam and foundation. The foundation block was modeled using contact surfaces to represent a continuous bedding plane parting forming the block base plane (termed EP3), side planes formed by faults that diverge in the downstream direction (fault F4 on the lower down-slope side and fault F1 on the upper upslope side), and a back release boundary formed by a series of joints that closely follow the upstream face of the dam. This block was selected as the critical block based on the results of numerous uncoupled analyses.

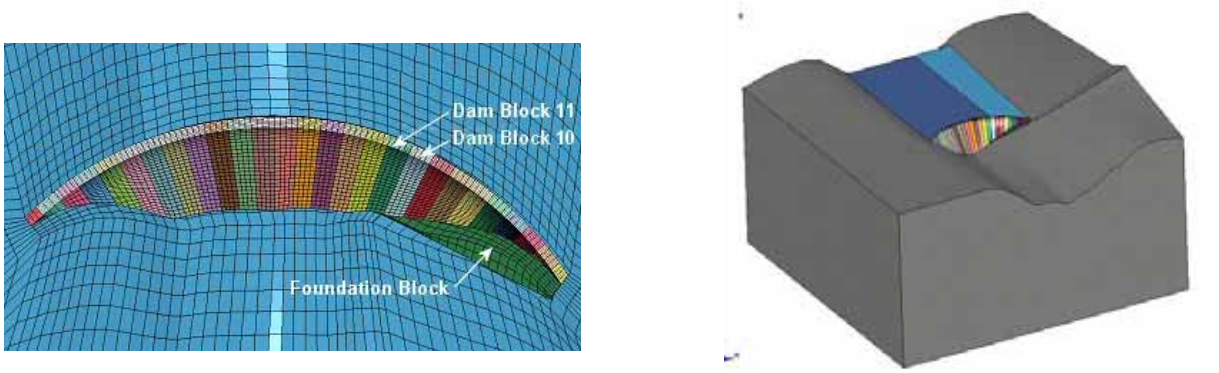

Figure 2. LS-DYNA finite element model

1.2.2 Calibration and Verification Studies

A considerable amount of effort went into calibrating and verifying the LS-DYNA model. The first order of business was to ensure that the model could predict the failure mode being studied while maintaining all appropriate loading; in this case sliding of the left abutment foundation block while maintaining the reservoir load. Of particular concern was the interaction of the modeled contact surfaces where they intersect in the vicinity of the rock block, and the behavior of the reservoir elements where they contact the dam and foundation. To test the model's performance, all contraction joint and block plane friction angles were set to zero. Drilling and digital borehole imaging showed the contact between the dam and foundation to be well bonded. For this reason, this contact was tied with appropriate tensile and shear strength values. The exception to this was the contact between dam Block 10 and the foundation. Because the lower rock block side boundary (F4) cuts diagonally across the foundation of this monolith, it was not clear what resistance this contact might provide. Therefore, the friction angle at the base of Block 10 was also set to zero for the test run. Displacements, contact surface normal forces for all moving contacts, and energy terms were tracked during application of static loads with the reservoir at normal maximum, elevation 3560.

Not surprisingly, it was discovered that the rock block actually moved along the theoretical intersection between a vertical contraction joint adjoining dam Blocks 10 and 11, and the base plane (EP3), with separation at fault F4, as shown greatly exaggerated (displacements multiplied by 100) in Figure 3. In addition, the base of dam Block 10 remained in contact with the rock block, but lifted off the adjacent foundation surface. Since the dam Block 10-11 contraction joint converges with fault F1 in a downstream direction, movement would ultimately be restrained. Very little information was available about fault F1, and existing exposures at the site were extremely limited. Therefore, F1 was removed from the solution, such that it did not provide constraint to downstream sliding (the down-slope side of the F1 contact surface was allowed to penetrate into the up-slope side). In addition, it was found that in order to maintain reservoir load (and well-behaved reservoir elements) during displacement of the block, a sliding contact surface was needed longitudinally through the reservoir, lining up with the upstream edge of the contact surface between dam Blocks 10 and 11. The contact surfaces between the reservoir water and the dam, and between the reservoir bottom and water upstream of the rock block also needed to be sliding surfaces. This necessitated careful evaluation during seismic loading to ensure the water did not separate significantly at these contact surfaces. The type of contact surface employed also proved to be important. Surfaces with "tie-break" options did not work well when only friction was specified. There tended to be an initial large perturbation in the response as these surfaces adjusted to the loading. The contact between the reservoir bottom and water was tied elsewhere. With this arrangement, the block moved out smoothly, while maintaining the reservoir loading at appropriate hydrostatic levels.

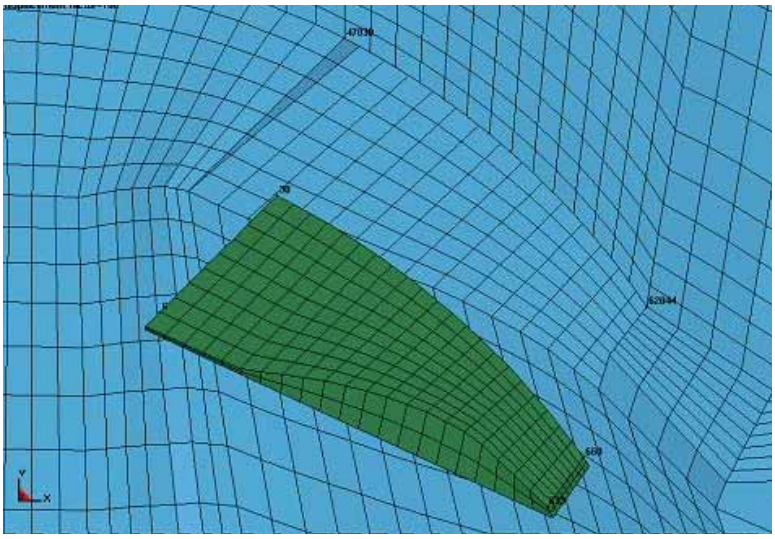

Figure 3. Displacement of rock block with zero friction, magnified 100 times

Additional verification studies included: (1) comparing the acceleration of the block calculated by the program for the sliding portion of the model under zero friction and a known resultant force to the theoretical acceleration from F = ma, (2) demonstrating that sliding initiates at a known force consistent with the frictional resistance, and (3) confirming that sliding contact shear forces were no greater than the normal force multiplied by the tangent of the contact friction angle. These tests were all considered necessary to ensure there were no inappropriate constraints in the model, and that the predicted displacements were not unduly restricted. The tests for F = ma were run without damping.

The model was calibrated using results from forced vibration testing, ambient vibration testing, testing performed on 6-inch-diameter concrete cores taken from the dam, and density measurements of the rock and concrete. With the contact surfaces tied, a velocity pulse was applied to the model at depth. Nodal velocities were extracted along the crest of the dam and evaluated using a Fourier analysis. The frequencies extracted in this manner were compared to the measured values. The modulus values for the dam and foundation were adjusted until a reasonably good match was found between the measured and calculated frequencies, while keeping the concrete modulus within the range measured in the lab. Using this approach, the concrete modulus was estimated to be $6x10^6$ lb/in^2 (approximately the average value from static uniaxial compression testing), and the foundation modulus $7x10^6$ lb/in^2 (about 80 percent of the mean geophysical modulus value). The frequency comparisons are shown in Table 1.

Table 1. Comparison of measured and calculated frequencies (Hz)

Mode ->	1	2	3	4
Measured ->	2.67	3.54	4.44	5.37
Calculated ->	2.68	3.54	4.95	5.60

Care was taken in de-convolving the surface free field earthquake ground motions for input in the model at depth below the dam, along a layer of nodes just above the base of the model. Initial de-convolved motions, obtained from the seismologists, were applied to the LS-DYNA model of the foundation without the dam. The response of nodes at the ground surface (approximately mid-abutment) was captured, and the response spectra for the motions at these nodes were compared to the spectra for the original surface motions. Adjustments were made until close agreement was obtained.

1.2.3 Foundation Shear Strength

Direct shear testing of large diameter bedding plane parting and fault samples helped establish the shear strength of the foundation discontinuities, in conjunction with surface profile roughness evaluation. The basic friction angle was determined by subtracting the dilation from the sliding strength results. This subtracted the influence of sample roughness, and corrected for any alignment issues of the sample within the shear box. A straight line was fit through the data at low normal stress, forcing it through the origin (zero apparent cohesion). This resulted in a basic friction angle of about 32 degrees for EP3. A Rengers analysis was performed on bedding plane profiles collected using digital photogrammetry techniques, defining a “waviness” angle as a function of “base step length”, or horizontal distance measured along the profile. A base step length equal to about 1 percent of the sliding plane length was used to estimate the appropriate waviness angle, in this case equal to about 5 degrees. This was added to the basic friction angle to arrive at 37 degrees for the base plane. Although less important to the results since sliding did not occur along these features, a friction angle of 35 degrees was assigned to fault F4 based on testing samples of similar fault material, 40 degrees was used for the friction angle of fault F1 (when it was included in the analysis) since it appeared to be slightly stronger, and a friction angle of 45 degrees was assigned to the back release boundary to represent rough clean planar joints.

1.2.4 Foundation Water Forces

Water forces acting on the foundation block planes (and the base of dam Block 10) were calculated by superimposing foundation water total head contours (Powell et al, 2008) onto the finite element mesh. The

data (from temporary foundation drain piezometers, deep gallery piezometers, and downstream water levels) indicate the foundation water levels drop rapidly to the line of drains and then drop below the bedding plane partings before they daylight downstream. The vertical distance between the water surface and each submerged nodal point on the block planes defines the pressure head at that nodal point. The average pressure head acting over a contact element surface (defined by four nodal points) was calculated and a corresponding uniform pressure was applied over the element surface.

Two additional foundation water conditions were considered to represent expected post-earthquake water forces. Water forces could increase under such conditions if movement occurred, due to opening of the back release boundary and fault F4, and dilation of the base plane (EP3). Some drains may be offset by such seismic displacement. Therefore, one of the additional water pressure distributions was based on assuming full hydrostatic pressure along the upstream release planes, decreasing linearly to zero at the downstream edge of the block. The second assumed the drains remained 50 percent effective, with the water pressures again extending to the downstream edge of the rock block.

1.2.5 Concrete Strength

Concrete used at the upstream and downstream faces of the dam was considerably stronger (compressive strength about 2,000 lb/in^2 higher at 1 year) than the interior concrete. From recent testing of concrete core, exterior concrete placed near the faces of the dam exhibits an average compressive strength of over 8,000 lb/in^2, while the interior concrete exhibits an average compressive strength of about 4,900 lb/in^2. Static splitting tension tests on interior concrete, which are considered to be the most reliable test result for the purposes of estimating tensile and shear strength values, produced an average tensile strength of about 610 lb/in^2. The dynamic tensile strength of the parent concrete was taken to be 50 percent higher than the static splitting strength, or about 915 lb/in^2. The face concrete would have higher strength.

Due to the good bond between the concrete and foundation rock observed in all the drill core and digital borehole images, the contact was considered to be strong. The strengths of the dam-foundation contact were based on the average static concrete splitting tensile strength of 610 lb/in^2 from the laboratory testing. This value was adjusted using the following factors: 0.8 to account for direct tension across the contact, 0.85 to account for joint efficiency, and 1.5 to account for dynamic loading, based on the work of Cannon (1995). These factors result in a dynamic contact tensile strength value of about 620 lb/in^2. The shear strength cohesion was considered to be about 50 percent higher than the tensile strength, or approximately 930 lb/in^2. The finite element code assumes the contact surface is broken when the following criterion is satisfied:

$$\left(\frac{|\sigma_n|}{NFS}\right)^2+\left(\frac{|\tau|}{SFS}\right)^2\geq 1$$

Where, σ_n is the normal stress, NFS is the normal failure stress, τ is the shear stress, and SFS is the shear failure stress. If the normal stress is compressive, the first term is ignored. Thus, the frictional component of shear strength is not considered, which could be quite conservative when shear failures are predicted.

A friction angle of 37 degrees was included where the bond was broken, since on the left abutment the contact is formed by bedding planes and should have a similar friction angle. These strength values were assigned to the dam-foundation contact surfaces in the finite element model, except under Monolith 10 where no cohesion or tensile strength values were applied (only friction) between the dam and foundation, as previously described. However, the friction angle for the right abutment contact would be considerably higher due to the excavation surface breaking across bedding planes. A friction angle of 45 degrees was assigned to the vertical contraction joints between dam monoliths. This is considered to be very conservative, since shear keys, beveled at 45 degrees, were formed in the contraction joint surfaces.

1.2.6 Damping

Considerable attention was paid to the damping used in the dynamic analyses. Only Rayleigh mass proportional damping (α) was used. To ensure the system was not over-damped, which could lead to misleadingly small displacements, only a small value of α was used to ensure proper behavior of the reservoir elements. An α value of 1.8, which corresponds to 5.4 percent of critical damping at the fundamental frequency (excluding frictional damping provided by the sliding contact surfaces), was used during application of static loads until the system stabilized, then α was reduced to 0.5, which corresponds to about 1 to 2 percent of critical damping at the fundamental frequencies of interest for the dam, during application of the earthquake ground motions. Frictional damping along the contact surfaces was also present when sliding along joints occurred. Based on vibration decay from the pulse loading frequency calibration studies, the total damping was approximately 7 percent of critical. Inclusion of stiffness proportional damping was considered, but it slowed the computation time considerably, and there were concerns about the effects of stiffness proportional damping on sliding contact surfaces.

1.2.7 Analysis Results

Analyses were performed to estimate the factor of safety for the rock block under static conditions. The verified and calibrated model with fault F1 taken out of the solution was used for this purpose. The friction coefficients on all the sliding contact surfaces were reduced by a constant factor until sliding of the rock block occurred. The factor at which sliding just initiates is equivalent to the factor of safety. For existing uplift conditions, the factor of safety was determined to be greater than 1.5, and for the increased linear uplift condition, it was determined to be greater than 1.3

Dynamic analyses were run for 11 different synthetic ground motions based on fault rupture simulations; 3 at an estimated 10,000-year return period, 5 at an estimated 50,000-year return period, and 3 at an estimated 200,000-year return period. Small displacements of the rock block were calculated in all cases. The movements typically involve small downstream translations along the dam Block 10-11 contraction joint, with rotation of the block clockwise (looking down in plan) such that larger displacements occur at the upper end of the block (see Figure 4).

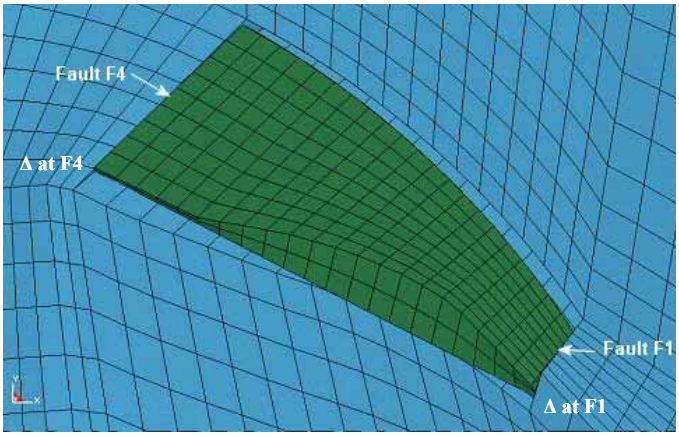

Figure 4. Displacements at the end of 50k gm5 magnified 100 times with fault F1 removed from solution

Deformation of the dam and rock resulted in development of positive normal forces along both fault F4 and the dam Block 10-11 contraction joint in many cases, although the normal force on F4 dropped to a small value as the contraction joint force increased and fault F4 tended to opened up, as shown in Figure 5. This allowed the described deformation pattern to occur whether fault F1 was included in the solution or not, although the displacements were reduced when F1 was included (as discussed further below). Complete separation at fault F4 occurred for the 200,000-year earthquake ground motions. A check of water forces against the dam monoliths upstream of the block showed that there was no significant reduction in loading as a result of the

movement, as shown in Figure 5.

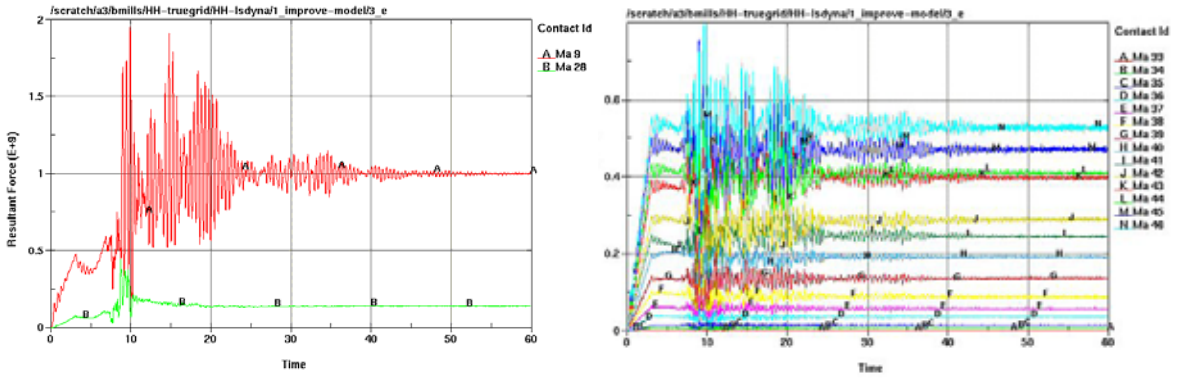

Figure 5. Normal forces on contraction joint between dam Blocks 10 and 11 (A) and fault F4 (B); and water forces acting on dam blocks upstream of the foundation block during 50k gm5

Table 2 shows the horizontal displacements at two locations on the block; (1) the downstream edge of the block at the down-slope end (fault F4), and (2) the downstream edge of the block at the up-slope end (fault F1), as shown in Figure 4. The vertical displacements were controlled by the bedding orientation such that contact between the rock block and underlying foundation was always maintained. Sensitivity studies were performed for the 50,000-year ground motion gm2 (the most critical of the 50k motions), first by including F1 in the solution, and then by further including the increased uplift with 50 percent drain efficiency that might result from block movement. The results, are shown in Table 2, indicate a slight decrease in movement when F1 is included, and a slight increase in movement with the increased uplift.

During the 200,000-year earthquake ground motion analyses, the dam separated from the foundation at several monoliths on the lower right abutment, with the contact strength being barely exceeded. This appears to be the result of large vertical velocity pulses in each of the ground motion records, and may have resulted in some re-distribution of loads and increased displacements.

Table 2. Dynamic Horizontal Rock Block Displacements (in)

Ground Motion	Conditions	Δ at F4	Δ at F1
Average 10k	No F1, Original Uplift	0.65	1.59
Average 50k	No F1, Original Uplift	0.96	2.37
Average 200k	No F1, Original Uplift	1.69	5.38
50k gm2	No F1, Original Uplift	1.42	3.19
50k gm2	F1, Original Uplift	1.32	2.68
50k gm2	F1, Increased Uplift, Drains 50% efficient	1.60	3.92

Previous physical shake table model studies on a typical arch dam indicated that the likely mode of failure is downstream rotation of blocks formed by propagation of horizontal cracking near the center of the downstream face and diagonal cracking parallel to the abutments through the structure as indicated by Payne, 2002. A check of dam stability showed large dynamic principal tensile stresses occurred in the dam near the center of the downstream face as shown in Figure 6, nearly aligned in the cantilever direction, but only for a small number of spikes (e.g. about 2 or 3 excursions greater than the estimated dynamic concrete tensile strength lasting fractions of a second each for the 50,000-year motions). Although this could result in localized horizontal cracking in this location, diagonal cracking parallel to the abutments and propagation of cracking through the structure would be required to initiate actual dam failure by block rotation. A check of maximum principal stresses closer to the abutment revealed significantly smaller maximum values, less than the tensile strength of the

parent concrete, as shown in Figure 6 for a typical 50,000-year earthquake. Maximum principal tensile stresses did not exceeded 700 lb/in^2 on the upstream face

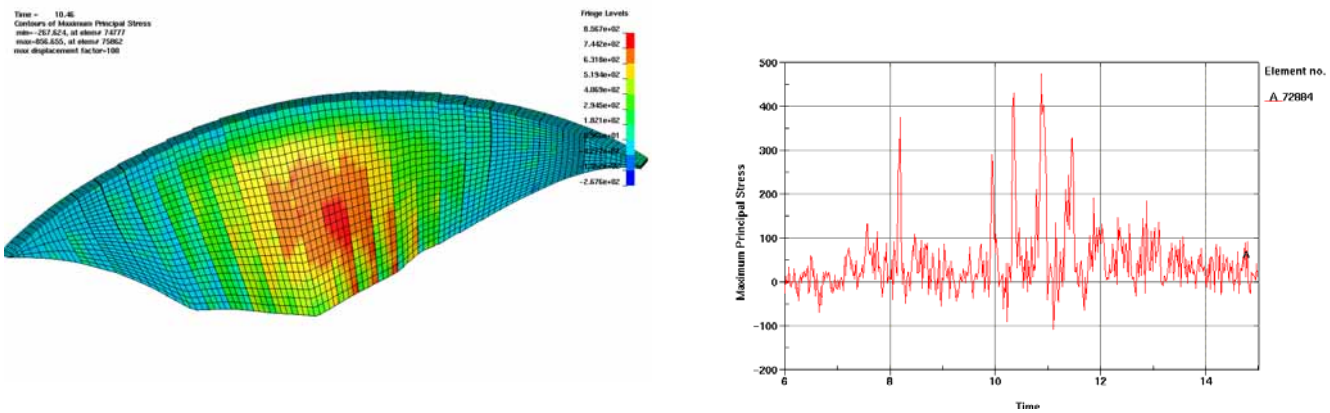

Figure 6. Maximum principal stress distribution on downstream face and maximum principal stress history for most highly stressed element toward abutment for 50k gm4

2. THIN ARCH DAM

The finite element model for the thin arch dam shown in Figure 7 has been analyzed for temperature loads. These analyses have indicated that the stability of the potential block in the foundation is dependent upon the temperature and reservoir elevation conditions. The dynamic analyses for this dam will be undertaken in the near future for a series of ground motions records and temperature/reservoir elevation combinations.

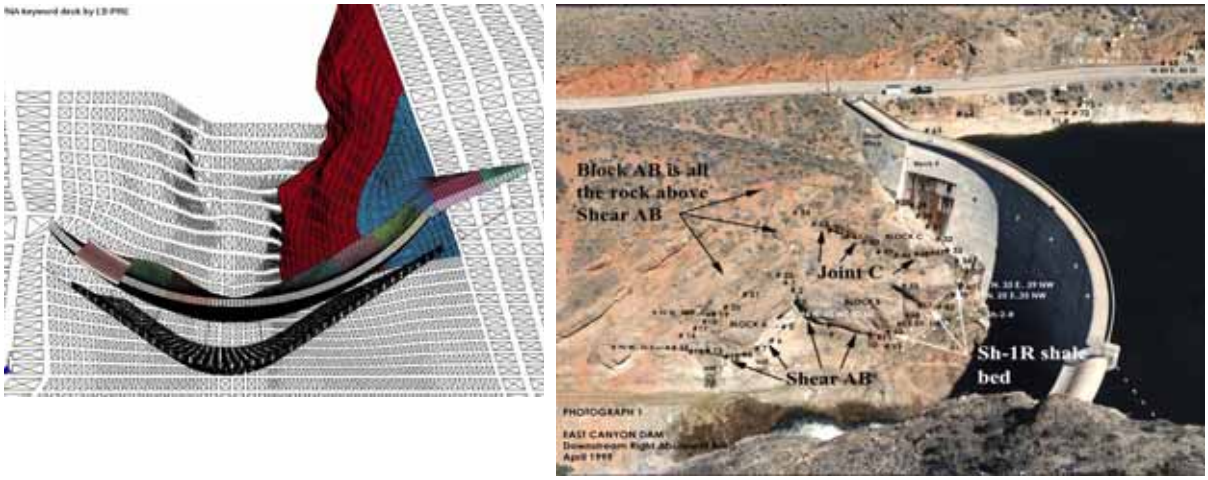

Figure 7 Finite element model of thin arch dam with foundation block and photograph of the dam and foundation

REFERENCES

Cannon, R.W. (1995), "Appendix E, Tensile Strength of Roller Compacted Concrete," EP 1110-2-12, U.S. Army Corps of Engineers, Washington, D.C.

Livermore Technology Software Corporation (2003), "LS-DYNA Version 970," Livermore, California.

Payne, T.L. (2002), "Shaking Table Study to Investigate Failure Modes of Arch Dams," *Proceedings, 12th European Conference on Earthquake Engineering*, London, U.K., paper 145.

Powell, C.N., P.T. Shaffner, and J. Wright (2008), "Hungry Horse Dam Stability - Geotechnical Input for Finite Element Model Studies," *Proceedings, United States Society on Dams Annual Meeting*, Portland, Oregon.